Paleoceanography

Supporting Information for

The Mechanistic Role of the Central American Seaway in a GFDL Earth System Model. Part 1: Impacts on Global Ocean Mean State and Circulation

Lori T. Sentman[1], John P. Dunne[1], Ronald J. Stouffer[1], John P. Krasting[1], J. R. Toggweiler[1], and Anthony J. Broccoli[2]

[1]National Oceanic and Atmospheric Administration/Geophysical Fluid Dynamics Laboratory, Princeton, New Jersey
[2]Department of Environmental Sciences and Institute for Earth, Ocean, and Atmospheric Sciences, Rutgers, The State University of New Jersey, New Brunswick, New Jersey.

Contents of this file

Introduction

The following supporting information contains text and figures which support the main article.

Text S1 includes extended GFDL-ESM2G model information relevant for the main article.

Figures S1 and S2a show published (Bell et al., 2015) paleoclimate oxygen **(S1)** and carbon **(S2a)** isotope proxy data from various Ocean Drilling Program (ODP) sites before and after the Central American Seaway shoaling and closure, supporting the motivation for this study. Figure S2b shows ODP site locations referenced in Figure S2a. Figure S3 shows published paleogeography reconstructions of Central America (Kirby and MacFadden, 2005; Haug et al., 2004) supporting this study’s experiment design. Figure S4 shows GFDL-ESM2G global average upper 2000-m ocean temperature time series for the four seaway simulations showing quasiequilibrium. Figure S5 shows the vertically integrated ocean current changes with the progression of the seaway shoaling and closure. Figure S6 illustrates the sea surface height anomaly (relative to the global mean) for GFDL-ESM2G driving the net water mass transport from the Pacific to the Atlantic. Figure S7 shows the zonal mean ocean heat and salt transport in GFDL-ESM2G. Figure S8 illustrates the GFDL-ESM2G precipitation rate minus evaporation rate difference between the three seaway experiments and the CLOSED simulation, supporting the local hydrological response in the ocean mean state.

Text S1. Extended model description of GFDL-ESM2G

The atmosphere component, AM2, uses a 2˚ latitude x 2.5˚ longitude horizontal grid and 24 vertical levels and is similar to the component used the GFDL CM2.1 climate model (Delworth et al., 2006). The land model, LM3.0 (Milly et al., 2014), exchanges water, energy and CO_2 between the land and atmosphere, and includes interactive, dynamic vegetation capable of simulating ecosystem dynamics in response to climate (Shevliakova et al., 2009). The ocean biogeochemical and ecological component is Tracers of Ocean Phytoplankton with Allometric Zooplankton code version 2.0 (TOPAZ2; Dunne et al., 2013). Atmospheric CO_2 tracer was restored annually and globally to the 1860 reference value of 286 ppm_v (i.e., a concentration-driven configuration) allowing realistic diurnal and seasonal CO_2 variability over land and reduced atmospheric CO_2 drift during the model spin-up. The ocean component uses an isopycnal vertical coordinate with a 1˚ horizontal grid increasing to ⅓˚ meridionally at the equator, tripolar above 65˚N, and 63 vertical levels, including two mixed layers (Hallberg, 2003; Thompson et al., 2003), two buffer layers, and 59 interior layers. To avoid excessively deep mixed layer depths (Hallberg, 2003), sub-mesoscale eddy-driven restratification of the mixed layer is parameterized after Fox-Kemper et al. (2011). The model uses Simmons et al. (2004) baroclinic tide mixing. The model uses the areal depth average of high-resolution bathymetry with the full sill depth and represents explicit exchanges across 14 straits.

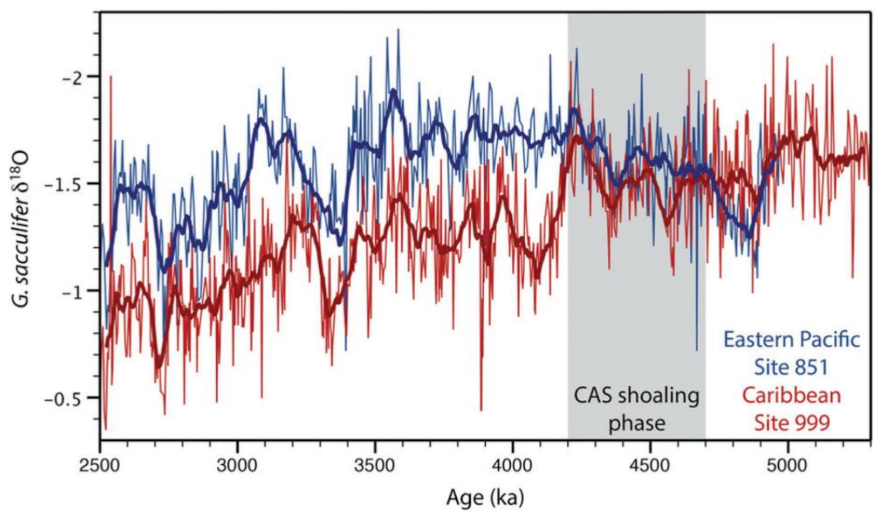

Figure S1. Comparison of surface water (planktic) oxygen isotope records (‰ vs Vienna Pee Dee Belemnite) from the Caribbean (ODP Site 999 (12°44′N, 78°44′W, Colombian basin; water depth 2828 m; Haug and Tiedemann, 1998) and the eastern Pacific (ODP site 851; 2°46′N, 110°34′W, water depth 3760 m; Cannariato and Ravelo, 1997) for 2.2-5.3 Ma showing an increased gradient between ~4.7-4.2 Ma attributed to a major shoaling phase of the CAS (grey shading), reprinted from "Atlantic Deep-water Response to the Early Pliocene Shoaling of the Central American Seaway" by Bell et al. (2015) licensed under CC-BY-4.0. Bold lines represent 50 kyr running averages (Haug et al., 2001; Figure 2A).

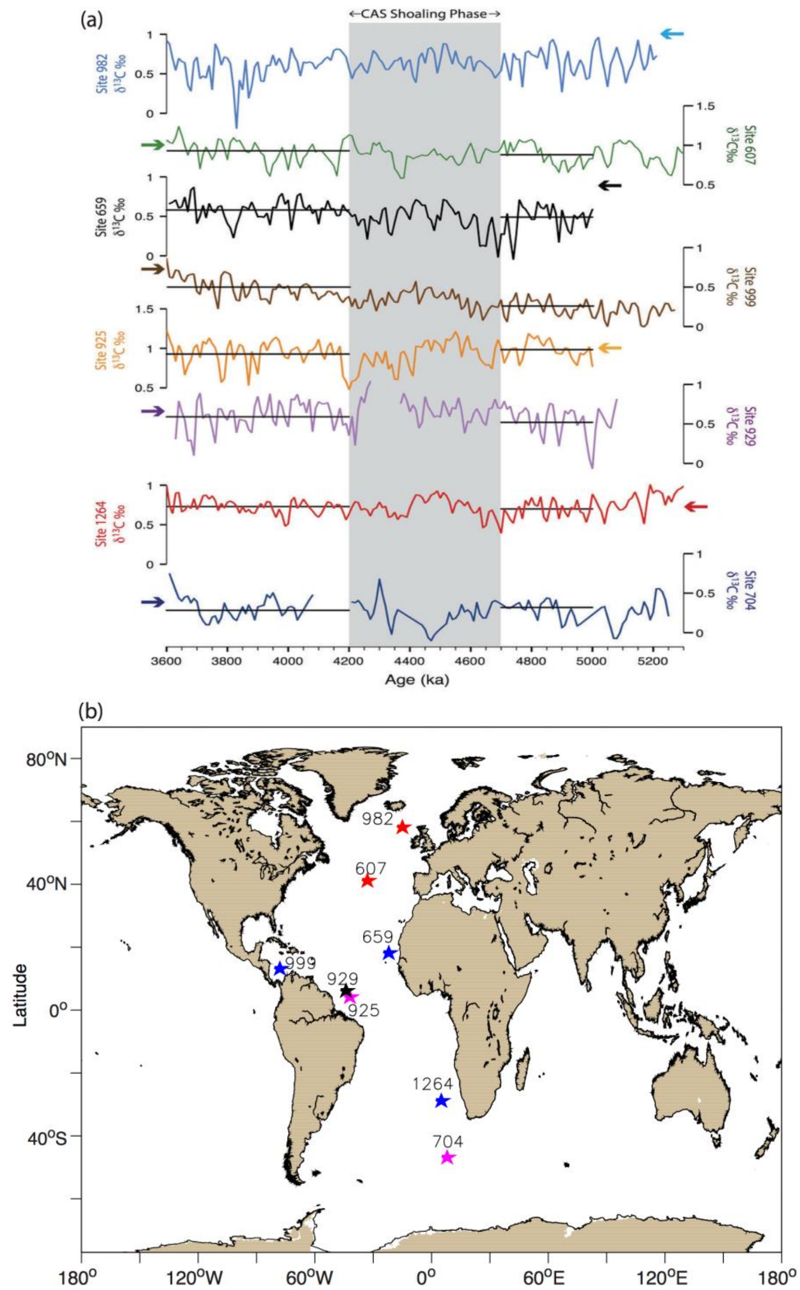

Figure S2. (a) Time series of δ13C data (‰ vs Vienna Pee Dee Belemnite) from various Atlantic ODP sites, reprinted from "Atlantic Deep-water Response to the Early Pliocene Shoaling of the Central American Seaway" by Bell et al. (2015) licensed under CC-BY-4.0. Horizontal black lines show average δ13C values for the time slice intervals prior to (5.0-4.7 Ma) and after (4.2-3.6 Ma)

CAS shoaling. Arrows indicate approximate modern δ13C values at each site. (b) Locations of Atlantic ODP sites from (a) represented by stars.

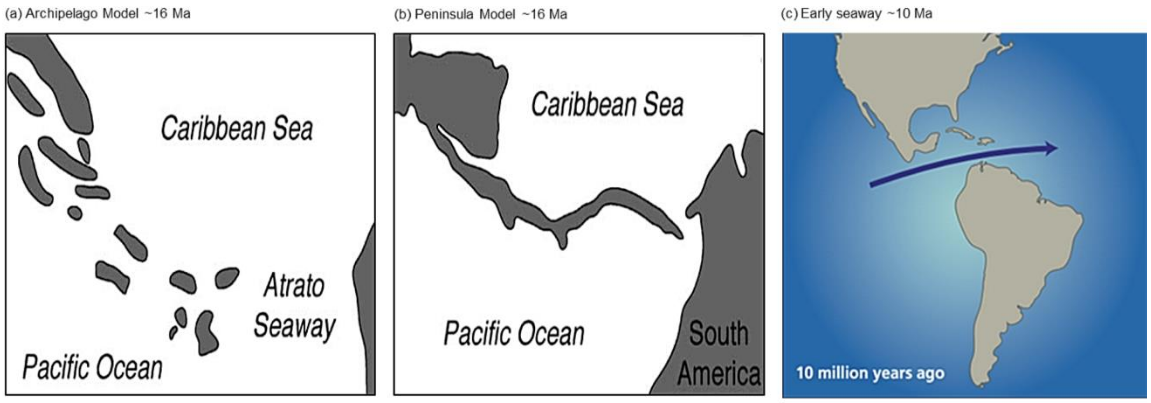

Figure S3. Paleogeography reconstructions of Central America in the mid-Miocene before the Isthmus of Panama; **(a)** archipelago model (Coates and Obando, 1996) reprinted from (Kirby and MacFadden, 2005) with permission from Elsevier[1], **(b)** peninsula model (Whitmore and Stewart, 1965) reprinted from (Kirby and MacFadden, 2005) with permission from Elsevier[1], and **(c)** early seaway model similar to previous climate model studies, republished with permission of *Oceanus Magazine*, from How the Isthmus of Panama put ice in the Arctic, G. H. Haug and L. D. Keigwin, 42, 2, 2004; permission conveyed through Copyright Clearance Center, Inc. Emergent land is represented by gray **(a)** and **(b)** and tan **(c)**. Timing and structure of the paleogeography is uncertain (Kirby and MacFadden, 2005). [1](a) and (b) reprinted from (*Palaeogeography*, *Palaeoclimatology*, *Palaeoecology*, M.X. Kirby and B. MacFadden. "Was southern Central America an archipelago or a peninsula in the middle Miocene? A test using land-mammal body size", Vol. 228, No. 3-4, p. 193–202, 2005, Copyright Elsevier) with permission from Elsevier.

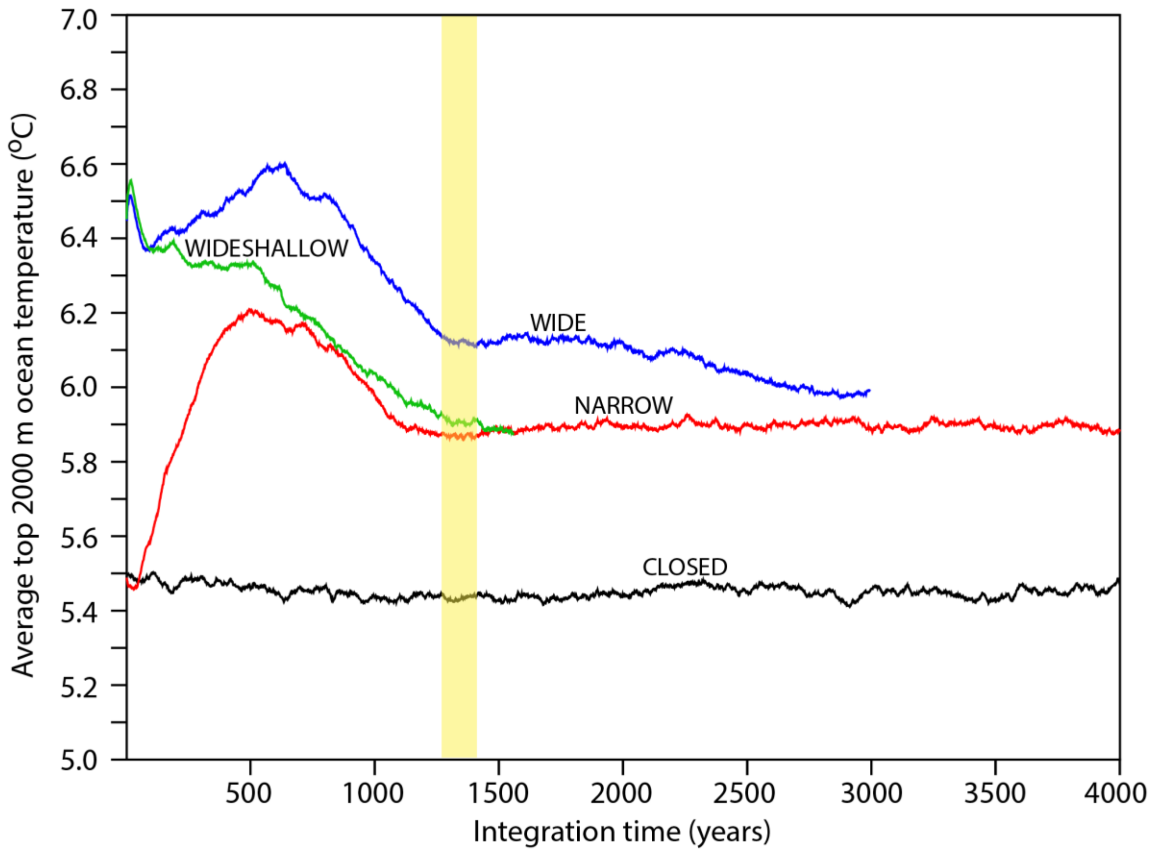

Figure S4. GFDL-ESM2G global average upper 2000-m ocean temperature (°C) for the CLOSED (black), NARROW (red), WIDESHALLOW (green), and WIDE (blue) seaway simulations for model integration years 1-4000. The yellow shading represents the 100-year analysis period (1301-1400) mainly used in this study (except for the maximum Atlantic Meridional Overturning Circulation analysis). The wide seaway experiments (e.g., WIDE and WIDESHALLOW) began with a warmer global integrated ocean and average surface air temperature than the NARROW seaway experiment because more land grid cells were replaced with warm, tropical ocean grid cells than in the NARROW seaway. The global average upper 2000-m ocean temperature for the WIDESHALLOW seaway converges toward the NARROW simulation faster than the WIDE simulation that was initialized with additional warm ocean grid cells. The NARROW and WIDE simulations were integrated longer than our spin-up and analysis periods to assess the convergence rate. The WIDE simulation converges toward the NARROW simulation at a rate of approximately 0.1˚C / 1000 years, requiring an additional 1000 integration years for near-convergence.

106

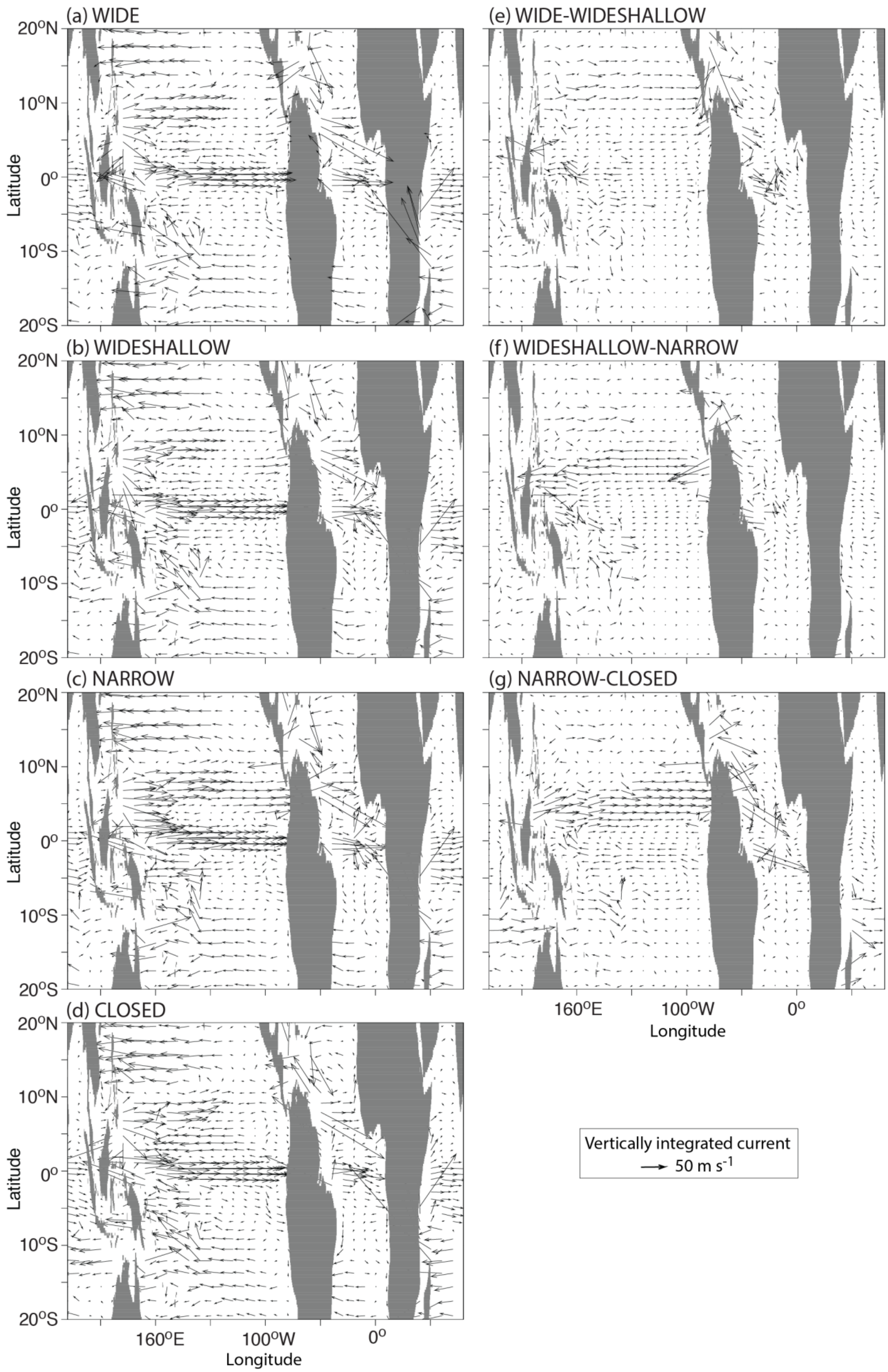

(a) WIDE
(b) WIDESHALLOW
(c) NARROW
(d) CLOSED
(e) WIDE-WIDESHALLOW
(f) WIDESHALLOW-NARROW
(g) NARROW-CLOSED
20ºN
10ºN
0º
10ºS
20ºS
Latitude
160ºE
100ºW
0º
Longitude
Vertically integrated current
50 m s-1

Figure S5. GFDL-ESM2G 100-year annual average vertically integrated full-depth current (m s^{-1}; vectors) from 20ºN to 20ºS for **(a)** WIDE, **(b)** WIDESHALLOW, **(c)** NARROW, **(d)** CLOSED, and the time progression of the gradual shoaling and closure of the seaway: **(e)** WIDE-WIDESHALLOW, **(f)** WIDESHALLOW-NARROW, and **(g)** NARROW-CLOSED differences.

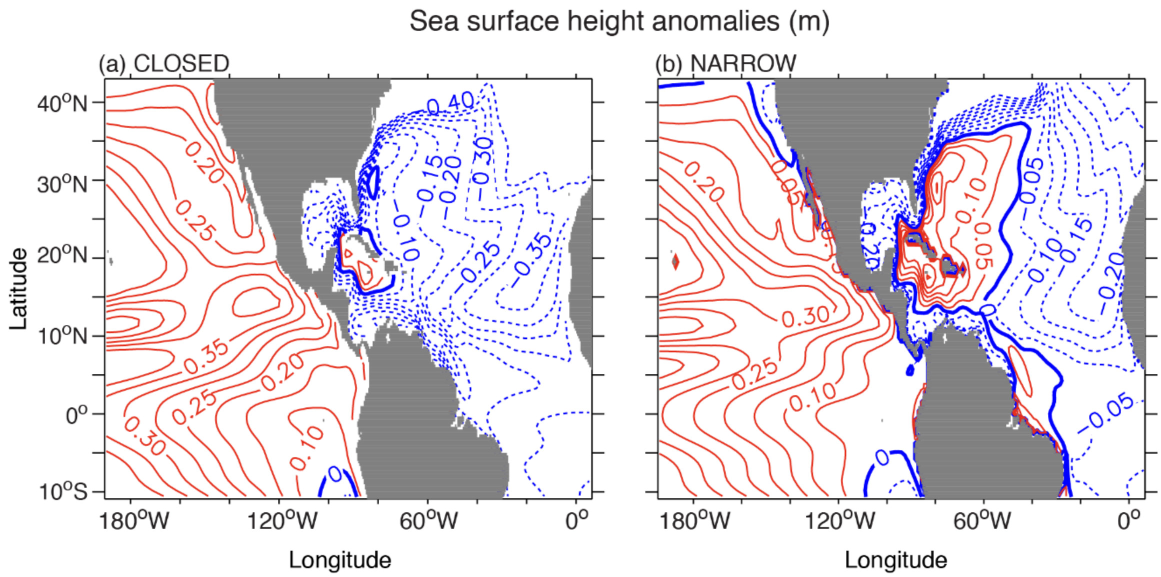

Figure S6. GFDL-ESM2G sea surface height (SSH) anomalies (m) relative to the global mean for the **(a)** CLOSED and **(b)** NARROW seaway simulations. Red (blue) contours indicate positive (negative) SSH anomalies. SSH anomalies for WIDESHALLOW and WIDE at steady-state were similar to NARROW but were not included in this analysis because these experiments were initialized differently with respect to SSH.

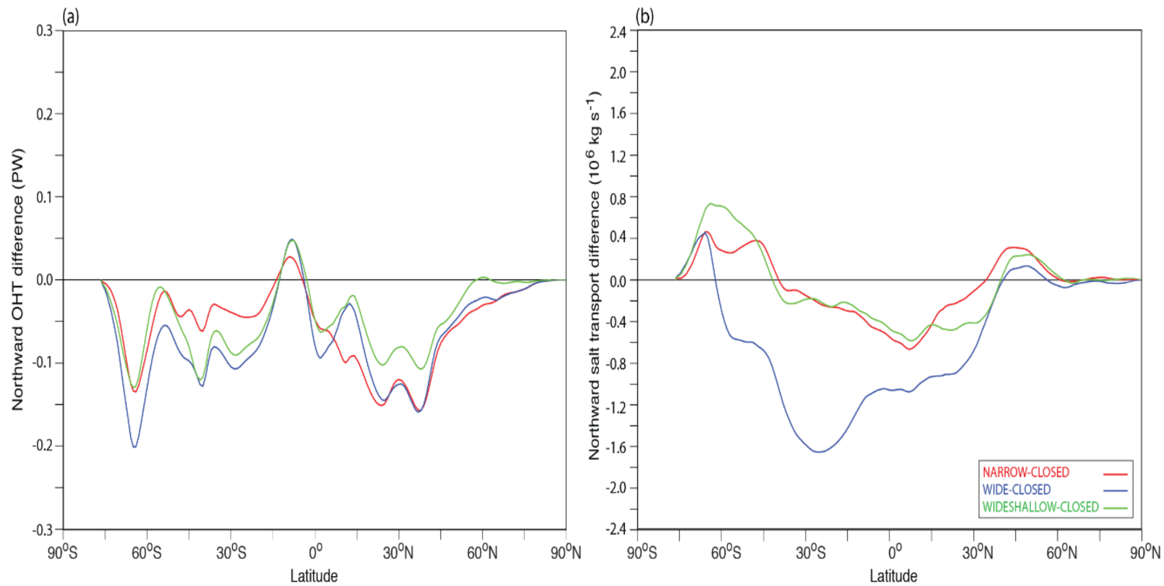

Figure S7. GFDL-ESM2G 100-year annual average NARROW (red), WIDE (blue), and WIDESHALLOW (green) minus CLOSED northward **(a)** ocean heat transport (PW) and **(b)** salt transport (10^6 kg s^{-1}) difference.

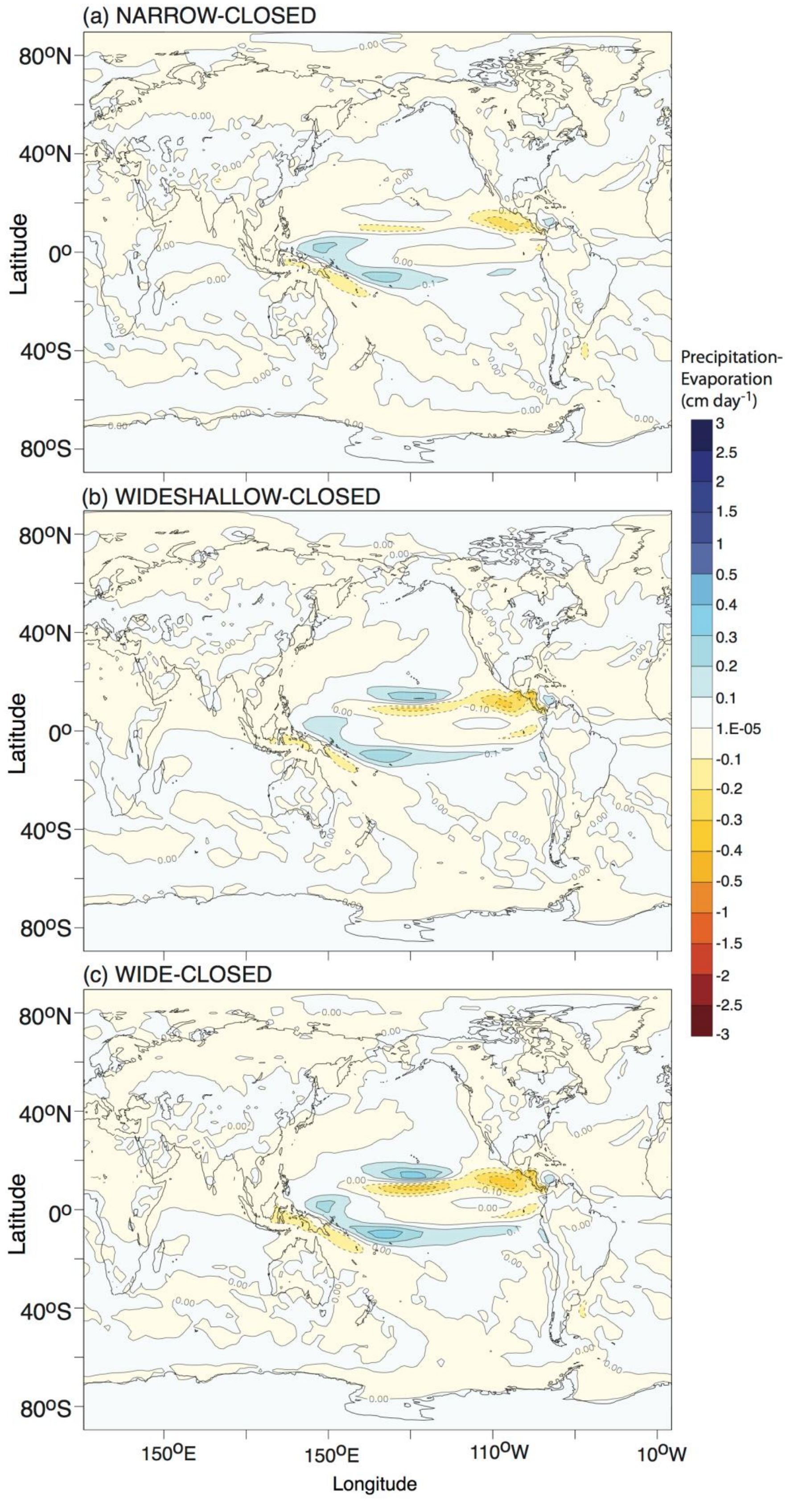

(a) NARROW-CLOSED
(b) WIDESHALLOW-CLOSED
(c) WIDE-CLOSED
80ºN
40ºN
0º
40ºS
80ºS
Latitude
150ºE
150ºE
110ºW
10ºW
Longitude
Precipitation-
Evaporation
(cm day⁻¹)
3
2.5
2
1.5
1
0.5
0.4
0.3
0.2
0.1
1.E-05
-0.1
-0.2
-0.3
-0.4
-0.5
-1
-1.5
-2
-2.5
-3

125

Figure S8. GFDL-ESM2G 100-year annual average precipitation rate minus evaporation rate (cm day^{-1}) for **(a)** NARROW-CLOSED, **(b)** WIDESHALLOW-CLOSED, and **(c)** WIDE-CLOSED. Positive (negative) values represent increased surface moisture (drying) with a CAS.